Deconvolving Current from a Faraday Rotation Measurement

Stephen E. Mitchell, Member, IEEE

Manuscript received December 20, 2006. This manuscript has been authored by National Security Technologies, LLC, under Contract No. DE-AC52-06NA25946 with the U.S. Department of Energy. The United States Government retains and the publisher, by accepting the article for publication, acknowledges that the United States Government retains a nonexclusive, paid-up, irrevocable, worldwide license to publish or reproduce the published form of this manuscript or allow others to do so, for United States Government purposes.

S. E. Mitchell is with National Security Technologies, LLC, P.O. Box 98521, Las Vegas, NV 89193-8521 (e-mail: mitchese@nv.doe.gov).

Abstract—In this paper, a unique software program is reported which automatically decodes the Faraday rotation signal into a time-dependent current representation. System parameters, such as the Faraday fiber's Verdet constant and number of loops in the sensor, are the only user-interface inputs. The central aspect of the algorithm utilizes a short-time Fourier transform, which reveals much of the Faraday rotation measurement's implicit information necessary for unfolding the dynamic current measurement.

Index Terms—Faraday rotation, STFT, Mega-amps, Verdet

INTRODUCTION

The pulsed power community and power generation industry is finding increased applications utilizing Faraday effect sensors. The Faraday effect in single-mode fibers permits fast-responding current sensing on high-voltage, high-current transmission lines [1]-[4]. The underlying theory of how the Faraday effect works is best described in the quantum mechanical realm, but can be understood on a basic classical electrodynamics level [5]. Various Faraday current sensing configurations along with subtle Faraday effects, which may adversely affect the system, are described elsewhere [6]. In typical configuration, linear polarized light launched into a Faraday current fiber emerges with a rotating linear polarization state at an angular frequency proportional to dI/dt. The axis of polarization of this emerging light is usually preadjusted through a half-wave plate and then split into two differently oriented analyzers such as the Wollaston beam splitter, which conveniently splits the beam and orients the polarization orthogonal to each other. The emerging light out of each facet or analyzer is optically modulated and captured via typical optical-electrical photodetectors and digitizers. If the orientation of the analyzers are orthogonal, optically modulated signals proportional to $\mathrm{Sin}^2[\theta(t)+\phi]$ and $\mathrm{Cos}^2[\theta(t)+\phi]$ (or $\frac{1}{2}\{1-\mathrm{Cos}(2[\theta(t)+\phi])\}$ and $\frac{1}{2}\{1+\mathrm{Cos}(2[\theta(t)+\phi])\}$, respectively) are produced where the angle, $\theta(t)$, is manifested from the Faraday effect within the fiber medium while the angle, ϕ, is some initial starting phase dependent on the half-wave plate and the state of polarization of the Faraday fiber itself. It may be convenient to orient the analyzers at 0° and 45° relative to the horizontal to yield optically modulated signals proportional to $\frac{1}{2}\{1+\mathrm{Cos}(2[\theta(t)+\phi])$ and $\frac{1}{2}\{1\pm\mathrm{Sin}(2[\theta(t)+\phi])$. In this case, a basic post processing technique is to subtract off the DC offset in each signal and take the ratio of such signals to yield a $\mathrm{Tan}(2[\theta(t)+\phi])$ like wave form which indicate increases or decreases in $\theta(t)$. The current, I(t), is directly proportional to the Faraday rotation angle, $\theta(t)$, through the simple closed-form equation

$$\theta(t) = VLB(t) = \mu_o VN'I(t) = V'N'I(t) \qquad (1)$$

where B(t) is the time-dependent magnetic field produced from the dynamic current, I(t), along the closed path, L as defined in Ampere's law for typical cylindrical symmetric systems. The parameter, N′, is the product term of the number of current paths (i.e., electrical windings) and the number of Faraday fiber loops in the sensing region. The Verdet constant, V, is redefined in more convenient units of radians/amps or radians/mega-amps. This is accomplished by multiplying the permeability of vacuum constant, μ_o, and redefining the product, $\mu_o V$, as the new Verdet constant, V′, used throughout the rest of this paper.

For some experiments, simply counting each full apparent Faraday rotation up to an identifiable turnaround point (i.e., in the current representation, the point in which the current is either a maximum or minimum) within the recorded Faraday rotation signal is sufficient in determining the peak current within some allowable fringe uncertainty. For many other experiments, a higher demand for unfolding the entire dynamic current profile is required. In such cases, investigators often rely extensively on user interaction on the Faraday rotation data by visually studying the data for crucial cues and identifiers, which will eventually represent the X-Y data points of the current measurement. After the often tedious process, a piece-wise, $\Delta I/\Delta t$, representation of the current may be revealed with the proviso of having a known reliable Verdet constant of the Faraday fiber or medium.

This work reports a unique method for uncovering the current measurement by utilizing a short-time Fourier transform (STFT), which basically is a Fourier transform over a windowed section of a signal to reveal frequency content as it changes over time. STFT details are discussed elsewhere [7]. However in this particular application, the STFT is used to uncover details necessary for transforming a single Faraday rotation signal into a current measurement representation and by using only a fraction of the optical components. The emerging rotating linear polarized light is not split and analyzed directly, thus bypassing the half-wave plates, beam splitters, polarizers, and possibly other associated and complementary optical components. Needless to say, this translates to tremendous cost savings (more than several thousands of dollars), especially during explosive-driven pulsed power applications in which most equipment is likely to be expended.

DETAILED DESCRIPTION

Traditional method basics

Before detailing the novel method of deciphering a Faraday signal into a useful current representation, a review of unfolding current from a Faraday signal via traditional methods may be useful. As an example, a simulated current shown in Fig. 1 produces a pair of Faraday signals which are optically decoded modulated signals proportional to $\frac{1}{2}\{1\pm\sin(2[\theta(t)+\phi])\}$ and $\frac{1}{2}\{1+\cos(2[\theta(t)+\phi])\}$ for analyzers at 45° and 0° relative to the horizontal, respectively. These signals are shown separately for clarity in Fig. 2 and 3, respectively, as signal A and B elsewhere throughout this paper. The angle, ϕ, is some initial starting phase dependent on the half-wave plate and the state of polarization of the Faraday fiber itself. For clarity, Fig. 4 shows a close-up of the two superimposed Faraday signals in a particular region of interest. Fig. 5 indicates an example of a ratio of such signals with the prerequisite DC offset subtracted out to yield a $\tan(2[\theta(t)+\phi])$ like signature wave form, which also indicates increases or decreases in $\theta(t)$.

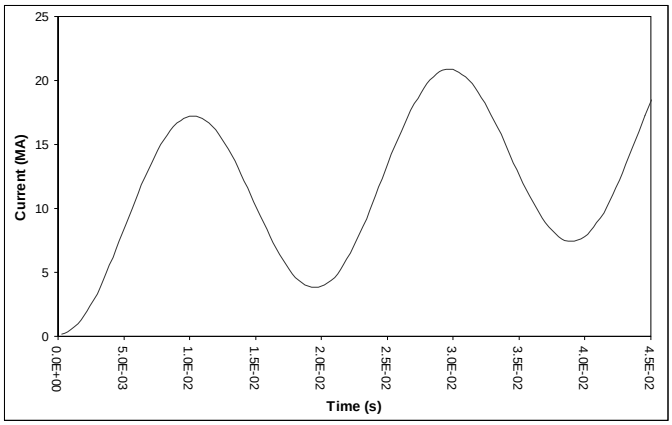

Fig. 1. Computer simulated current.

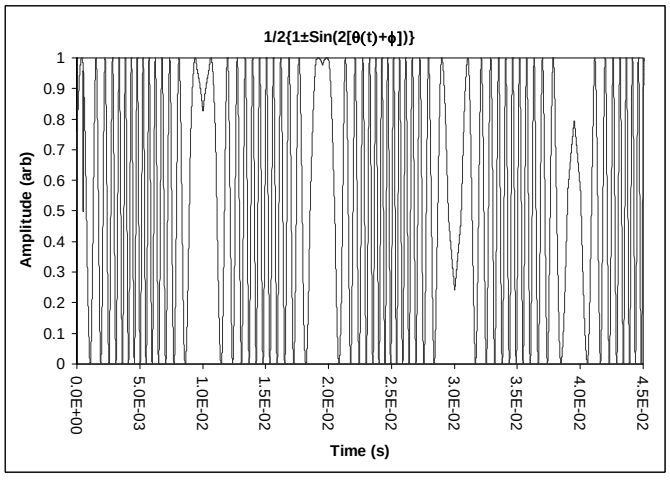

Fig. 2. Simulated Faraday decoded signal proportional to $\frac{1}{2}\{1\pm\sin(2[\theta(t)+\phi])\}$.

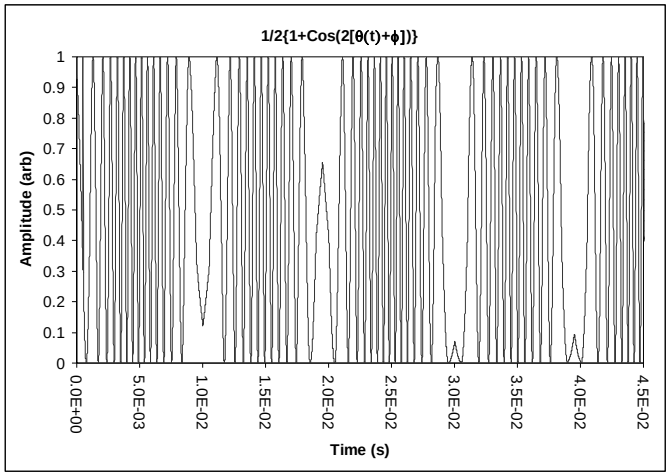

Fig. 3. Simulated Faraday decoded signal proportional to ½{1+Cos(2[θ(t)+ϕ])}.

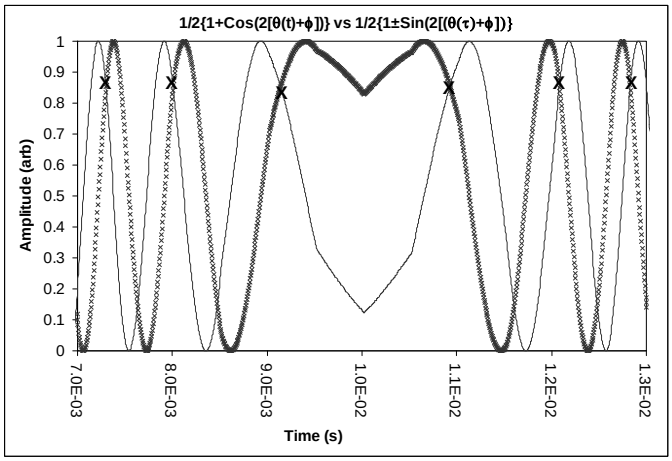

Fig. 4. Windowed region of interest of superimposed simulated Faraday signals to show leading and lagging aspects before and after a "turn-around" point. This point coincides with a local extrema in the current representation. The bold "X" marks are indicators for times in which signal A crosses signal B during each observed complete Faraday rotation.

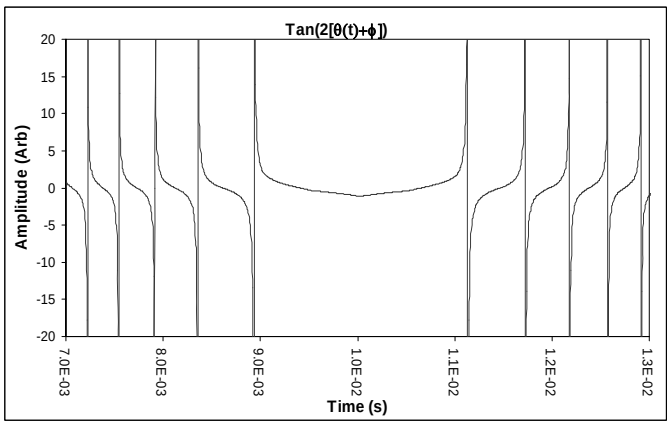

Fig. 5. Same windowed region of interest indicating the ratio of the signals which yields a Tan(2[θ(t)+ϕ]) like signature wave form.

Note the qualitative nature of how one signal leads the other before the turnaround and then reverses (lags) itself past the turn-around point. These are all telling signs of a current signal at its local extrema value. A piece-wise current representation may now be reconstructed from these observed leading/lagging crossing points. Starting with (1), current I(t) can be expressed in terms of θ(t) as follows:

$$I(t) = \frac{\theta(t)}{N'V'} \tag{3}$$

But I(t) can be expressed as a sum of $\Delta I(t_n)$ where t_n are the individual times at which signal A either leads or lags signal B at its corresponding crossing times. These individual times, t_n , coincide with the bold "X" marks represented in Fig 4. $\Delta I(t_n)$ is further defined as

$$\Delta I(t_n) = \frac{\Delta\theta(t_n)}{N'V'} = \frac{\Delta\theta(t_n)}{\Delta t_n}\frac{\Delta t_n}{N'V'}, \tag{4}$$

where the observed time period, Δt_n, corresponds to the nth occurrence in which the Faraday signal appears to have undergone a 2π radian rotation or one full revolution (aka "fringe") during a time difference, $t_{n+1} - t_n$. However, the rotation only appears to have undergone a 2π radian rotation due to the trigonometric double angle identity typically associated with Faraday rotation signals as discussed in the introduction, and therefore, requires an additional division by two to get back $\theta(t)$. Thus, for every fringe, an incremental change in current, $\Delta I(t_n)$, is

$$\Delta I(t_n) = \left(\frac{2\pi}{2N'V'\Delta t_n}\right)\Delta t_n = \left(\frac{\pi}{N'V'\Delta t_n}\right)\Delta t_n \tag{5}$$

where $\pi/N'V'\Delta t_n$ is the piece-wise $\Delta I/\Delta t_n$ segment. The sum of each of these $\Delta I/\Delta t_n$ segments times each adjacent Δt_n given in (6), represents the total piece-wise reconstructed current shown in Fig. 6.

$$I(t) = \sum_n^N \left(\frac{\Delta I}{\Delta t_n}\right)\Delta t_n = \sum_n^N \left(\frac{\pi}{N'V'\Delta t_n}\right)\Delta t_n \tag{6}$$

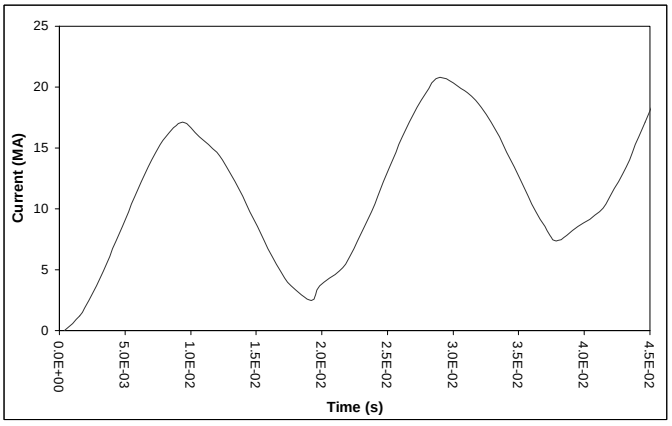

Fig. 6. Piece-wise reconstructed current representation from a pair of Faraday optically decoded modulated signals.

New method

Starting with (5), $\Delta I(t_n)$ is rewritten as $\Delta I(t_m)$ to denote a time, t_m, different from that previously defined and will be explained in the paragraphs to follow. To begin, $\Delta I(t_m)$ can also be expressed in terms of a frequency, ν_m, as

$$\Delta I(t_m) = \frac{\pi}{N'V'}\left(\upsilon_m \Delta t_m\right) \tag{7}$$

where the frequency, ν_m, is inversely proportional to the Δt_n term in the denominator of (5) where Δt_n corresponds to the time period of the nth observed Faraday rotation cycle. However, in the new method, the frequency, ν_m, is determined by a Buneman frequency estimator algorithm [8] over a STFT whose window's time span is fixed and begins at time, t_m. The Buneman frequency estimator algorithm is a unique method of calculating the fundamental frequency of a windowed portion of a signal that may not be exactly sinusoidal or periodic. The window's time span should be at least as large as the largest time period, Δt_n, observed for the traditional method discussed from the previous section. Section IV of this paper discusses window types, time

spans, and references further information regarding these topics. The STFT is subsequently shifted in time by a fixed incremental amount, $\Delta t_m = t_{m+1} - t_m$, and the next succeeding frequency, ν_{m+1}, is determined. The incremental time, Δt_m, is typically smaller than the smallest observed time period, Δt_n, recorded from the traditional method and could be comparable to the recording instruments sampling time. This process continues throughout the signal record producing a frequency response versus time representation. Fig. 7 shows the frequency response with respect to time of Faraday signal shown in Fig. 2. In this representation, the local extrema, which reflects both maximas and minimas in the current, are clearly shown where the frequency, ν, goes to zero (i.e., $\Delta\theta/\Delta t = 0$). Likewise, the inflection points are represented by the maximum frequency values. For each successive extrema pair (e.g., maxima to minima or minima to maxima) in time, there is an intermediate inflection point whose sign alternates. By programmatically changing the sign of every other inflection group, the converted frequency response shows both positive and negative frequencies that are increasing and decreasing, respectively. This result is displayed in Fig. 8. Integrating this corrected representation of the Faraday frequency response corresponds precisely to the Faraday rotation angle changing direction through local extrema in the current representation. After multiplying by the scaling constant, $\pi/N'V'$, the final unfolded current is revealed in Fig. 9.

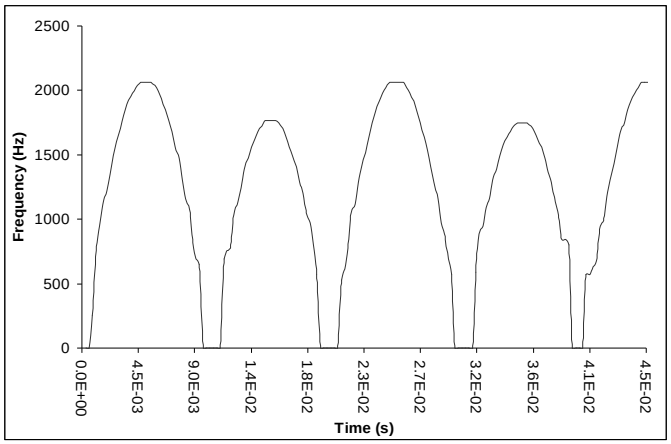

Fig. 7. Faraday signal's uncorrected frequency response with respect to time.

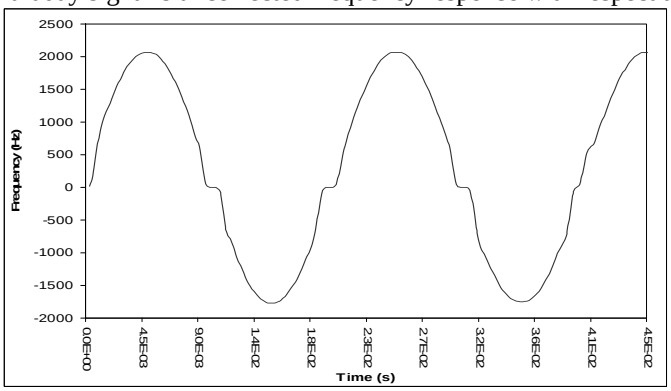

Fig. 8. Faraday signal's converted frequency response with respect to time which is directly proportional to $\Delta\theta/\Delta t$.

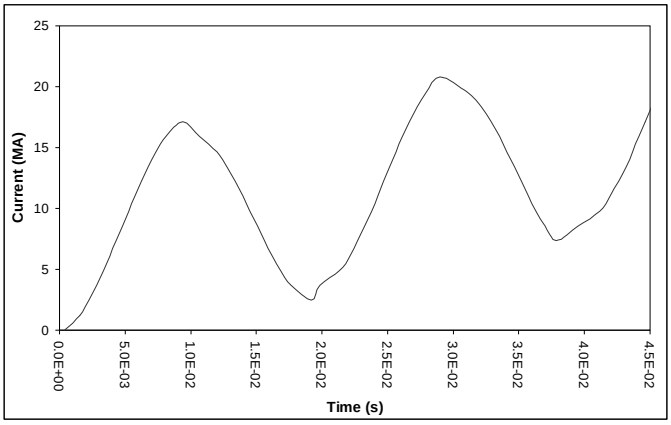

Fig. 9. Integrated Faraday signal's converted frequency response with respect to time. The scaling factor is precisely defined in terms of the Verdet constant and the generalized amplification term.

RESULTS

Verifying the accuracy of the new method of deconvolving a dynamic current representation from a Faraday rotation measurement requires a quantitative measure of correlation. Correlation [9] in this regard is a figure of merit relating how well one data record compares to another. Such verification is most often preferred rather than a qualitative visual validation as shown in Fig. 10. However, due to widely varying time disparities between data points for all methods described herein, the record lengths of the standard versus the new unfolded current record also differ. Thus, resampling either one of the two records using a basic cubic spline interpolation algorithm [10] to achieve equal length data sets was necessary prior to any correlation analysis.

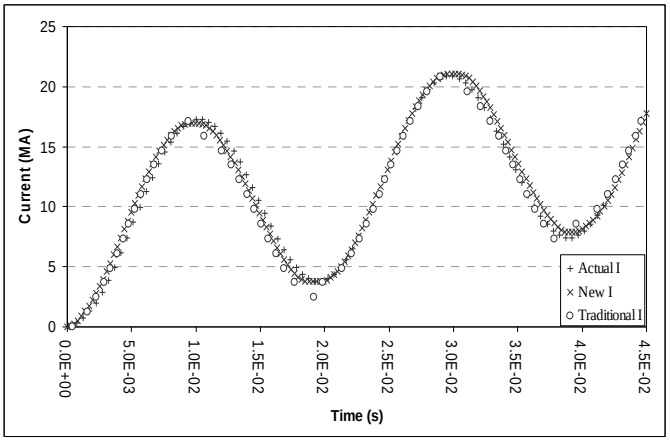

Fig. 10. Overlay of the actual current "+", the traditional method of current decoding "o", and the new method of current decoding "x".

After resampling either one of the two records to achieve equal length data sets, a correlation could be achieved between the two record sets through the following relation

$$C(X,Y) = \frac{N\sum_{i=1}^{N} X_i Y_i - \sum_{i=1}^{N} X_i \sum_{i=1}^{N} Y_i}{\sqrt{N\sum_{i=1}^{N} X_i^2 - \left(\sum_{i=1}^{N} X_i\right)^2}\sqrt{N\sum_{i=1}^{N} Y_i^2 - \left(\sum_{i=1}^{N} Y_i\right)^2}} \quad (8)$$

where, C(X,Y) is the correlation factor between record arrays X and Y, where X represents the actual current measurement array elements while Y represents the array elements from either method of current measurement. Correlation values range between 0 and 1 inclusively; whereas a correlation value of 1 represents perfect correlation while a value of 0 represents no correlation.

The correlation values produced from the traditional and new methods are 0.96 and 0.99, respectively. In this case, the new method offers an approximate 3 percent improvement over the traditional method with potential cost savings of several thousands of dollars in optical components, fabrication, and assembly expenses per Faraday rotation sensor.

New method used on real experimental data

The new method was used on Faraday rotation data recorded from two different pulsed power sources. One record set was from a Lawrence Livermore National Laboratory designed, National Security Technologies, LLC, built 10kV 10kA 22kJ capacitive discharge bank and another record set from the Nevada Test Site-operated ATLAS pulsed power facility.

22kJ capacitive discharge bank

In a particular experiment, the bank discharged its electrical energy into a 350μH solenoid load consisting of 50 electrical coil turns. A 30-loop Faraday fiber sensor was configured into the load so that a portion of each fiber loop ran parallel and axially through the center of the load and return path loop around the outside load. This setup provided a good test of what was earlier referred as generic amplifying factor, N′. In this case, the generic amplifying factor, N′, is 30 x 50 = 1500. The Verdet constant of the Faraday fiber was known to be 2.55 rad/MA at an operating laser source wavelength of 850 nm. A typical Faraday rotation signal produced is shown in Fig. 11 from one such bank discharge.

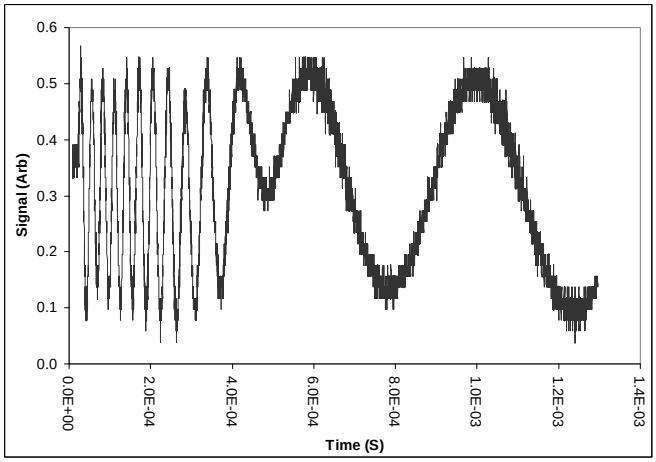

Fig. 11. Faraday rotation signal resulting from discharging the 22kJ capacitive storage bank into a specially configured load.

A qualitative comparison is shown in Fig. 12 which compares the bank's calibrated Pearson probe current measurement with the new method of current measurement from a Faraday rotation signal. Quantitative comparison of the new method of current measurement with the Pearson probe's current measurement indicated a correlation of 0.97.

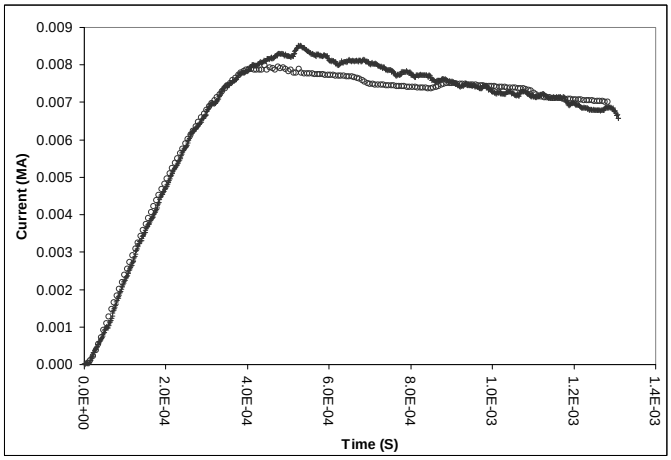

Fig. 12. "x" represents the Pearson probe current measurement. "o" represents the new method of current measurement from a Faraday rotation signal.

ATLAS pulsed power facility

A single loop Faraday fiber sensor was configured concentrically about the central current carrying output load conductor. The Verdet constant of the Faraday fiber was known to be 2.68 rad/MA at an operating laser source wavelength of 830 nm. A typical Faraday rotation signal produced from the ATLAS pulsed power facility is shown in Fig. 13. A qualitative comparison is shown in Fig. 14 which compares the ATLAS's current measurement with the new method of current measurement from a Faraday rotation signal. Quantitative comparison of the new method of current measurement with the ATLAS data indicated a correlation of 0.99.

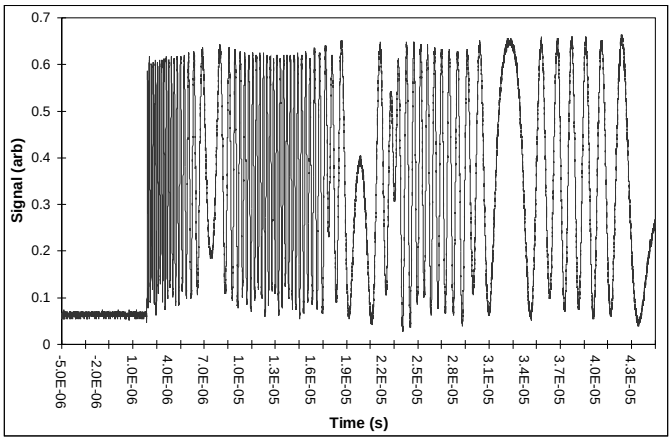

Fig. 13. A typical Faraday rotation signal resulting from one of the many ATLAS pulsed power experiments.

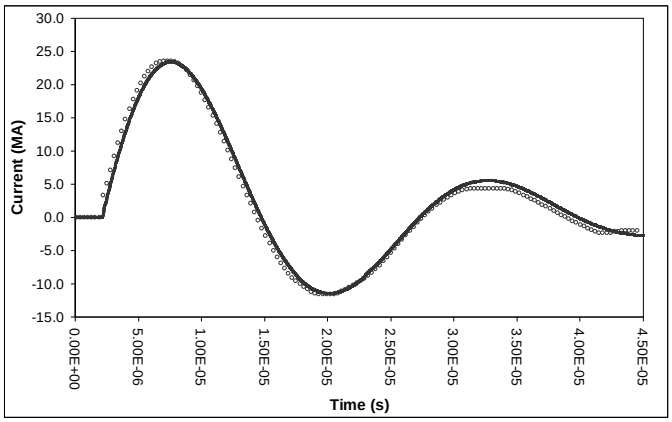

Fig. 14. The solid line represents the current measurement made from the traditional method using a host of associated optical components, which produced a pair of quadrature decoded Faraday rotation signals. "o" represents the new method of current measurement from a single, quadrature decoded-free Faraday rotation signal.

Software Program

The software algorithm was developed using the LabView 7.1 program [11]. The program's graphical user interface is shown in Fig. 15. Prior to running the program, the user updates each of the relevant user-input fields, such as the Verdet constant or amplifying factor (i.e., the Gain as indicated on the interface). Depending on what format the Faraday rotation signal data were recorded, the user may also select either comma-separated-variable or Tab delimitated options.

A challenging aspect of using the program is inputting effective 'Time Step Fraction' and the 'Time Window Fraction' values. The 'Time Step Fraction' refers to the incremental time shift in which the STFT window sequentially shifts through the entire Faraday signal record. This time increment divided by the total time of the record represents the fraction. A small time increment produces a greater resolved current reconstruction, but generally at the expense of greater computational processing time. Trade-offs between resolution and computational time may be weighed [12] and details discussed elsewhere [13]. However, this is not an issue due to powerful gigahertz processing and gigabyte RAM capabilities commonly available on computers of today's era.

Spectral leakage is a primary concern associated with STFT's. Spectral leakage represents unnecessary high frequency content and may impair the Buneman frequency estimation in a particular windowed region of the signal. High frequency content present in the frequency-domain may be attenuated by imposing a special window function with tapered end points in the time-

domain prior to the Fourier transform as opposed to an unspecified or rectangular windowed region. The choice of window type and length are also discussed in detail elsewhere [14] for other applications. However, a Hanning window type with time span comparable to the period of the slowest frequency in the data record yields sufficient results. The window's time length divided by the total time of the record represents the 'Time Window Fraction' input value also located on the user interface. A simple block diagram of the code's algorithm is illustrated in Fig. 16.

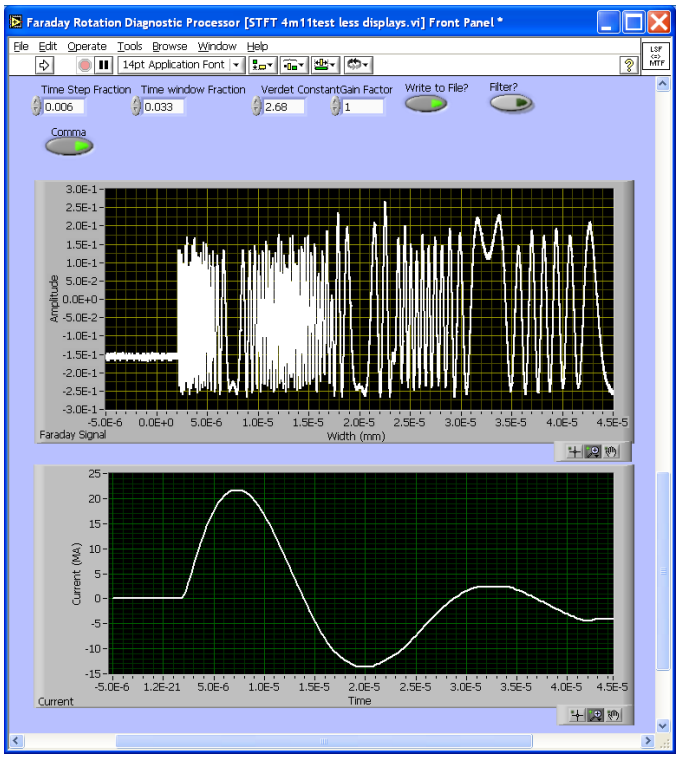

Fig. 15. The graphical user interface to the program developed for processing a current measurement from a Faraday rotation signal.

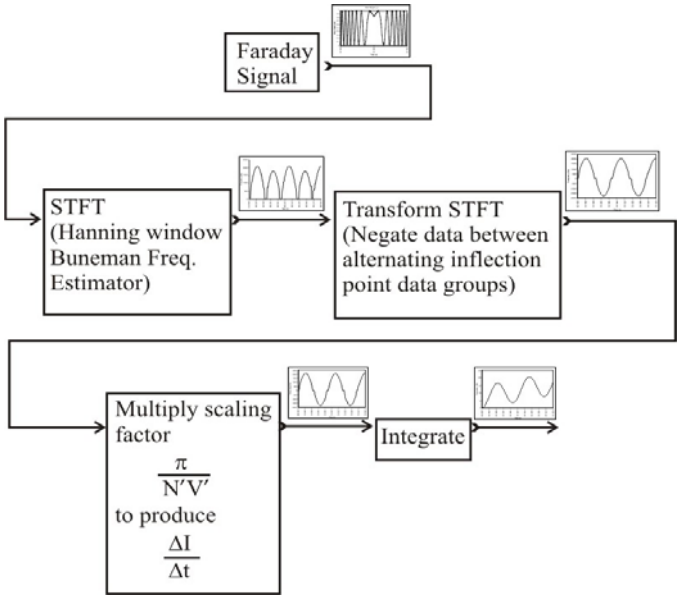

Fig. 16. Illustration to visualize signal flow process from one process to the next. The description of each functional block description is discussed further in section II.B of this paper.

Conclusion

The new method reported herein this paper demonstrates a viable economical alternative method of determining a dynamic current measurement from a Faraday rotation signal. The new method produces an equivalent, or better, measurement compared

to a traditional method which generally requires costly optical components, packaging, and setup typical for quadrature decoding of a Faraday rotation signal. Such cost savings may be significant in explosive-driven pulsed power applications in which case most equipment may be expended.

ACKNOWLEDGMENT

The development of this technique was inspired and motivated by many people. I wish to thank Dave Goerz, Dave Reisman, and Stephen Fulkerson of Lawrence Livermore National Laboratory. Also, many thanks to Ed Utiger, Ed McCrea, Lynn Veeser, and Bruce Marshall of National Security Technologies, LLC, for their continued support and encouragement.

References

[1] S. C. Rashleigh and R. Ulrich, “Magneto-optic current sensing with birefringent fibers,” Appl. Phys. Lett. 34 (11), 1979, pp. 768.
[2] L. R. Veeser, G. I. Chandler, and G. W. Day, “Fiber optic sensing of pulsed currents,” Photonics: High Bandwidth Analog Application, SPIE 648, 1986, pp. 197.
[3] A. M. Smith, “Polarization and magneto-optic properties of single-mode optical fiber,” Appl. Opt. 17, 1978, pp. 52.
[4] F. J. Wessel, N. C. Wild, H. U. Rahman, A. Ron, and F. S. Felber, “Faraday rotation in a multimode optical fiber in a fast rise-time, high magnetic field,” Rev. Sci. Instrum. 57 (9), 1986, pp. 2246.
[5] E. Hecht and A Zajac, Optics, Addison-Wesley Publishing Company, Inc., 1979, pp. 262.
[6] A. M. Smith, “Birefringence induced by bends and twist in single-mode optical fiber,” Appl. Opt. 19 (15), 1980, pp. 2606.
[7] J. B. Allan and L. R. Rabiner, “A unified approach to short time Fourier analysis and synthesis,” Proc. IEEE 65, 1977, pp. 1558.
[8] D. H. Bailey and P. N. Swarztrauber, “The fractional Fourier transform and applications,” Society for Industrial and Applied Mathematics Review, 33 (3), 1991, pp. 394.
[9] K. Pearson, “Mathematical contributions to the theory of evolution. III. Regression, heredity and panmixia,” Phil Trans R Soc. Lond., Series A (187), 1896, pp.253.
[10] W. H. Press, S. A. Teukolsky, W. T. Vetterling, and B. P. Flannery, Numerical Recipes in C, the Art of Scientific Computing, Second Edition, Cambridge University Press, 1992, pp. 113.
[11] LabVIEW 7.1, National Instruments, Austin, TX, 2004.
[12] A. W. Peevers, “A real time 3D analysis/synthesis tool based on the short time Fourier transform,” M.S. Thesis, Dept. Elec. Eng., U.C. Berkeley, CA, 1994.
[13] X. Serra, “A system for sound analysis/transformation/synthesis based on a deterministic plus stochastic decomposition,” PhD Dissertation, Dept. Music, Stanford Univ., 1989.
[14] F. J. Harris, “On the use of windows for harmonic analysis with the discrete Fourier transform,” Proc. IEEE 66, 1978, pp. 51.